# An Explanation of Oscillations Due to Wind Power Plants Weak Grid Interconnection

Lingling Fan, *Senior Member, IEEE*, Zhixin Miao, *Senior Member, IEEE*

***Abstract*—An existing wind power plant at ERCOT experienced poorly damped and undamped voltage oscillations under weak grid conditions. The oscillations became worse during high power outputs. This letter aims to find the root cause of such oscillations. Our research provides a linearized system model by combining the vector control of wind power plants and the weak grid interconnection. Using this model, this letter succeeds in explaining that the weak grid condition introduces a zero in right half plane for the open-loop system, which can lead to poorly damped or undamped oscillations.**

***Index Terms*—Wind power plants, voltage oscillations, weak grids**

## I. Introduction

AN ERCOT wind power plant experienced poorly damped and undamped voltage oscillations under weak grid conditions [1]. The frequency of the oscillation is about 4 Hz. The oscillations are undamped at high power output and poorly damped at lower power output. The objective of this research is to provide a linearized system model to explain the possible root causes of such oscillations. Our approach is to develop a linearized system model by combining the vector control of wind power plants (WPPs) and the weak grid interconnection. Using this model, this letter will explain that weak grid condition introduces a zero in right half plane (RHP) for the open-loop system, which may lead to poorly damped oscillations at low power output as well as undamped oscillations at high power output.

## II. The System Model

The study system is illustrated in Fig. 1, where a WPP is connected to a grid through a transformer and a transmission line. The grid is modeled as a voltage source with a constant magnitude and a constant frequency. The total reactance from the WPP to the grid is $X$.

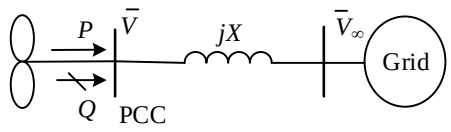


Fig. 1. The study system.

### The control block

In power system dynamic studies, a WPP is assumed to be a current source [2]. This assumption is also used in this letter. Further, the vector control of a WPP is based on a $dq$-reference frame, where the $d$-axis is aligned with the point of common coupling (PCC) voltage space vector. Details of converter vector control can be found in [3]. Therefore, we assume that the WPP can be represented by $dq$-axis currents: $i_d$ and $i_q$. The vector control of a power electronic converter has two cascaded loops: The outer real power/voltage loops track real power reference and the PCC voltage reference and generate current references $i_d^*$ and $i_q^*$; and the inner current loops track current references and generate the converter's output voltage $V_{td}$ and $V_{tq}$.

In this letter, we aggregate the detailed circuit dynamics related to the converter output voltage and the current, and current control dynamics into first-order systems with the current references as the inputs and the current measurements as the outputs. We assume that there is a time delay to realize current reference tracking. Though 20 ms is a typical value of the delay, during weak grid conditions, the effect of phase-locked-loop (PLL) will make the delay value longer [4]. The entire vector control now has power error and voltage error as the inputs and its outputs are $i_d$ and $i_q$.

### The plant model

*Currents to the PCC voltage*

We will first find the linearized relationship between the PCC voltage $\Delta V$ and the currents $\Delta i_d$ and $\Delta i_q$. Since the $d$-axis is aligned with the PCC voltage, therefore $v_d = V$ and $v_q = 0$.

In the $dq$-reference frame, the PCC voltage, current and grid voltage have the following relationship:

$$v_d + jv_q = (jX)(i_d + ji_q) + \bar{V}_\infty \tag{1}$$

Suppose that the PCC voltage is leading the infinity bus by an angle $\delta$. Then the above relationship becomes:

$$\begin{aligned} v_d &= -Xi_q + V_\infty \cos\delta, \\ 0 = v_q &= +Xi_d - V_\infty \sin\delta. \end{aligned} \tag{2}$$

Assuming that $\delta$ is within the range of $\{-\frac{\pi}{2}, \frac{\pi}{2}\}$, then

$$V_\infty \cos\delta = \sqrt{V_\infty^2 - (V_\infty \sin\delta)^2} = \sqrt{V_\infty^2 - (Xi_d)^2}. \tag{3}$$

Combining (3) and (2), we have:

$$v_d = -Xi_q + \sqrt{V_\infty^2 - (Xi_d)^2}. \tag{4}$$

Linearizing (4) leads to:

$$\Delta V = \Delta v_d = -X\Delta i_q - \underbrace{\frac{X}{\sqrt{\left(\frac{V_\infty}{Xi_d}\right)^2 - 1}}}_{c} \Delta i_d. \tag{5}$$

Lingling Fan and Zhixin Miao are with the Department of Electrical Engineering, University of South Florida, Tampa, FL 33420 USA e-mail: linglingfan@usf.edu.

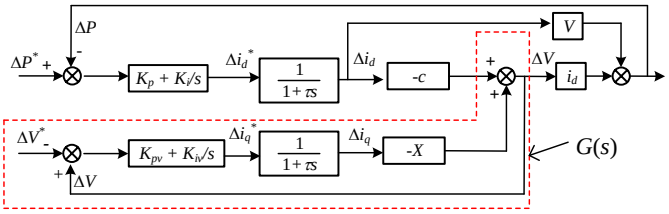


Fig. 2. Block diagram of the linearized system.

Note that $V_\infty/X$ is the short circuit current $i_{sc}$. The above equation shows that the PCC voltage will decrease when the output $dq$-axis currents from the converter increase. Further, if the $d$-axis current is increasing, or the real power output is increasing, the absolute value of the coefficient of $\Delta i_d$: $c$ will increase.

*Real power expression*

The real power by the WPP injected to the grid at the PCC bus is expressed as follows.

$$P = Vi_d \Longrightarrow \Delta P = i_d \Delta V + V \Delta i_d \tag{6}$$

The linear system model is shown in Fig. 2 by combining (6), (5), and the vector control blocks.

## III. Analysis

The closed-loop system in Fig. 2 has two feedback loops. First, the voltage loop is aggregated into a transfer function $G(s)$ as shown in Fig. 2. The system now has only one loop.

We use the root locus method to conduct stability analysis. The loop gain of the open-loop system is as follows.

$$L(s) = \frac{K_p\left(s + \frac{K_i}{K_p}\right)}{s} \frac{1}{1+\tau s} \underbrace{(V - ci_d G(s))}_{L'(s)}$$

where $G(s) = \frac{1}{1+\left(K_{pv}+\frac{K_{iv}}{s}\right)\frac{1}{1+\tau s}X}$.

$$L'(s) = V \frac{\tau(1-\frac{ci_d}{V})s^2 + (K_{pv}X + 1 - \frac{ci_d}{V})s + K_{iv}X}{\tau s^2 + (1+K_{pv}X)s + K_{iv}X} \tag{7}$$

Note that the loop gain has four poles: $0$, $-1/\tau$, and the two poles of $L'(s)$. The loop gain has three zeros. The first zero is related to the PI controller of the power loop $-K_i/K_P$. The two other zeros are the zeros of $L'(s)$. When $ci_d > V$, the coefficient of the quadrant term in the numerator of $L'(s)$ is negative. One zero will be located in the RHP. Note that $c$ is related to the system strength $X$ and $i_d$ or real power output. A weak grid indicates a large $X$ and hence a large $c$. High power output also indicates a large $c$. Fig. 3(a) gives a comparison of root loci for three different power outputs: 1.22 pu, 1.25 pu and 1.28 pu with $V = 1$ pu. By checking the gain when a root is at the imaginary axis, we can judge if the closed-loop system is stable ( if gain $\geq 1$) or unstable ( if gain $< 1$).

Fig. 3(b) presents the linear system simulation results for two cases. When $P = 1.26$ pu, the PCC voltage shows poorly damped oscillations. when $P = 1.27$ pu, the oscillations are undamped.

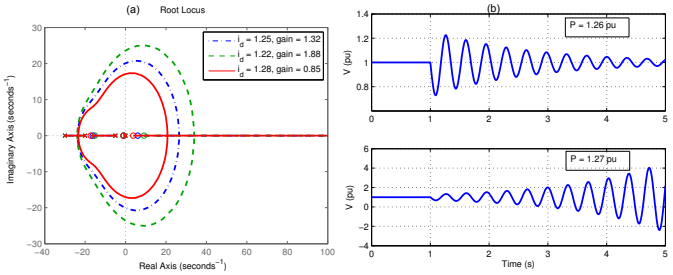


Fig. 3. (a) Effect of $P$ or $i_d$ on root loci. (b) Simulation results. When $i_d = 1.28$ pu, the closed-loop system is unstable. Other parameters: $\tau = 0.05$ s, $X = 0.75$, $K_p = 1$, $K_i = 1$, $K_{pv} = 1$, $K_{iv} = 10$, $V = v_d = 1$.

Sensitivity analysis is also conducted. The effect of the system strength $X$, power transfer level $P$, current control delay value $\tau$, and voltage controller's integral gain $K_{iv}$ on the closed-loop system's eigenvalues is shown in Fig. 4. It is observed that increasing those parameters leads to a less stable system.

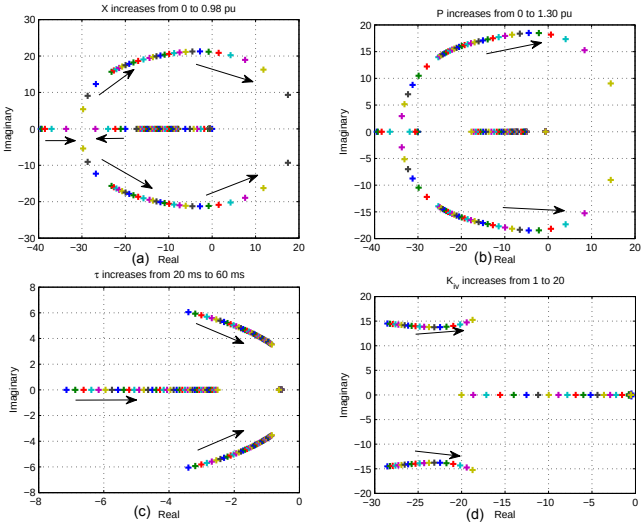


Fig. 4. Eigenvalue plots of the closed-loop system. (a) Effect of $X$; (b) Effect of $P$; (c) Effect of $\tau$; (d) Effect of $K_{iv}$. Base case parameters: $\tau = 0.05$ s, $X = 0.75$, $K_p = 1$, $K_i = 1$, $K_{pv} = 1$, $K_{iv} = 10$, $v_d = 1$, $P = 1$ and $Q = 0$.

## IV. Conclusion

A linear model combining weak system characteristics and WPP vector control is proposed. Using this model, we find the mechanism of oscillations: A RHP zero is introduced in the open-loop system due to weak grid interconnection. The research finding in this letter may be applicable to the voltage oscillations observed in ERCOT.

## References

[1] S.-H. Huang, J. Schmall, J. Conto, J. Adams, Y. Zhang, and C. Carter, "Voltage control challenges on weak grids with high penetration of wind generation: Ercot experience," in *Power and Energy Society General Meeting, 2012 IEEE*. IEEE, 2012, pp. 1–7.

[2] N. W. Miller, J. J. Sanchez-Gasca, W. W. Price, and R. W. Delmerico, "Dynamic modeling of ge 1.5 and 3.6 mw wind turbine-generators for stability simulations," in *Power Engineering Society General Meeting, 2003, IEEE*, vol. 3. IEEE, 2003, pp. 1977–1983.

[3] A. Yazdani and R. Iravani, *Voltage-sourced converters in power systems: modeling, control, and applications*. John Wiley & Sons, 2010.

[4] T. Midtsund, J. Suul, and T. Undeland, "Evaluation of current controller performance and stability for voltage source converters connected to a weak grid," in *Power Electronics for Distributed Generation Systems (PEDG), 2010 2nd IEEE International Symposium on*. IEEE, 2010, pp. 382–388.